Modulation of apolipoprotein B-100 mRNA editing: effects on hepatic very low density lipoprotein assembly and intracellular apoB distribution in the rat

Nicholas O. Davidson,[1,*] Ruth C. Carlos,[*] Helayne L. Sherman,[†] and Rick V. Hay[†]

Gastroenterology Section, Department of Medicine,[*] and Specialized Center of Research in Atherosclerosis, Department of Pathology,[†] University of Chicago, 5841 S. Maryland Avenue, Chicago, IL 60637

Abstract We have studied the consequences of alterations to hepatic apoB mRNA editing on the biosynthesis and intracellular distribution of newly synthesized apoB variants together with their mass distribution in nascent Golgi very low density lipoproteins (VLDL). Radiolabeled liver membrane fractions were prepared from control or hypothyroid animals and separated by discontinuous sucrose gradient centrifugation. Hepatic apoB-100 synthesis in these groups accounted for 93–100% of total newly synthesized apoB species of Golgi fractions recovered from the sucrose gradients (G_1 and G_2). The analogous fractions isolated from the livers of hyperthyroid (treated with 3,3',5-triiodo-L-thyronine, T_3) animals revealed that newly synthesized apoB-100 accounted for only 46 ± 10% (G_1) and 24 ± 11% (G_2), respectively, of total newly synthesized apoB. ApoB-100 mass in nascent Golgi VLDL from control and hypothyroid G_1 fractions represented 70–78% total apoB as determined by Western blot analysis. By contrast, Golgi VLDL from hyperthyroid animals contained predominantly (>78%) apoB-48 as the apoB species. Electron microscopy revealed that the morphology and size distribution of hyperthyroid G_1 VLDL were similar to particles isolated from control animals. Thus, despite a profound reduction in the proportion of apoB-100 mRNA species containing an unmodified codon (CAA, B-GLN) at position 2153 in hyperthyroid animals (6 ± 1% vs 50–61% in control and hypothyroid animals) apoB-100 biosynthesis was detectable in a defined membrane fraction isolated by discontinuous sucrose gradient centrifugation. However, no apoB-100 synthesis was detectable in liver samples prepared by Polytron disruption in Triton-containing buffers. These data suggest that effective hepatic VLDL assembly and secretion in the T_3-treated rat continues despite a profound reduction in apoB-100 biosynthesis and implies that apoB-48 contains the requisite domains to direct this process, a situation analogous to that in the intestine. —**Davidson, N. O., R. C. Carlos, H L. Sherman, and R. V. Hay.** Modulation of apolipoprotein B-100 mRNA editing: effects on hepatic very low density lipoprotein assembly and intracellular apoB distribution in the rat. *J. Lipid Res.* 1990. **31:** 899–908.

Supplementary key words nuclear thyroid hormone receptor • Golgi membranes • microsomal membrane subfractions • apoB-100 • apoB-48

Apolipoprotein B (apoB) is a large glycoprotein synthesized in mammalian enterocytes and hepatocytes as an obligate component of triglyceride-rich lipoproteins. In humans, apoB is synthesized in an organ-specific fashion with the liver elaborating a form of apparent M_r 549,000 referred to as apoB-100, while the intestine elaborates a form of apparent M_r 264,000 referred to as apoB-48 (reviewed in (1)). ApoB-48 is colinear with the amino terminal 2152 amino acids of apoB-100 arising from a unique posttranscriptional modification to the primary apoB transcript in which codon 2153 in apoB-100 cDNA is modified from CAA, encoding glutamine, to UAA, which encodes an in-frame translational stop codon (2, 3).

The rat differs from other mammals in that both forms of apoB are synthesized by the liver (4, 5). The molecular mechanism underlying production of these two distinct apoB variants in rat liver is identical to that described in human and rabbit intestine (6, 7) although the biological significance and physiologic implications of this species difference are unclear. In earlier studies it was demonstrated that rat hepatic apoB variants are heterogeneous with respect to both structural and metabolic properties in vivo (5, 8) and in particular demonstrate temporally distinct patterns of biosynthesis (9, 10). In addition, studies conducted using both rat liver perfusions and primary

Abbreviations: apo, apolipoprotein; VLDL, very low density lipoprotein; LDL, low density lipoprotein; PBS, phosphate-buffered saline; TTBS, Tris-buffered saline containing 0.05% Tween 20; SDS-PAGE, sodium dodecyl sulfate polyacrylamide gel electrophoresis; PVDF, polyvinylidene difluoride; PMSF, phenylmethylsulfonyl fluoride; EDTA, ethylenediaminetetraacetic acid, Na_2 salt; TLCK, N-α-tosyl-L-lysine-chloromethyl ketone; T_3, 3,3',5-triiodo-L-thyronine; PTU, (2-thio-4-hydroxy-6-n-propylpyrimidine); PCR, polymerase chain reaction, SSC (1 ×) 0.15 M NaCl/0.015 M Na citrate, pH 7.0.

[1]To whom correspondence should be addressed.

cultured hepatocytes suggest that intracellular processing and secretion of apoB variants may be independently regulated (9, 11). More recently, studies performed with cultured rat hepatocytes point to the existence of heterogeneous pools of apoB within the hepatocyte (12, 13) and raised the possibility that movement of nascent apoB species between specific compartments may become rate-limiting in the directed assembly and secretion of VLDL. Independent confirmation of these findings has emerged from studies of lipoprotein and apoB-100 assembly in HepG2 cells where it appears that nascent apoB-100 is cotranslationally bound to endoplasmic reticulum membranes and undergoes a progressive increase in neutral lipid content after its secretion into the microsomal lumen, findings that imply a step-wise process of VLDL assembly and secretion (14).

Recent studies from our laboratory have determined that hepatic triglyceride synthesis and secretion together with apoB biosynthesis are modulated in response to alterations in thyroid hormone status (15). These studies demonstrated a selective, profound decrease in apoB-100 biosynthesis, an effect subsequently shown (6) to result from hormonal modulation of the posttranscriptional apoB RNA editing mechanism. The hypothesis has therefore emerged that posttranscriptional RNA editing may represent an additional level of regulation of apoB gene expression in vivo. In order to characterize changes in hepatic VLDL assembly associated with hormonal modulation of apoB mRNA editing, we have analyzed the biosynthesis and intracellular distribution of newly synthesized apoB variants together with their mass distribution among microsomal membrane subfractions and nascent Golgi VLDL. The results suggest that hepatic VLDL assembly and secretion in the rat are effectively maintained despite profound reductions in apoB-100 biosynthesis and imply that apoB-48 may contain sufficient conformation properties to direct this process.

MATERIALS AND METHODS

Animals and treatment protocols

Male Sprague-Dawley rats were obtained from Charles River, Wilmington, MA in the weight range of 150 g. Animals were rendered hypothyroid after consumption of rat chow supplemented with 0.1% (w/w) propylthiouracil (2-thio-4-hydroxy-6-n-propylpyrimidine) (PTU) for 21–28 days as previously described and validated (15). Hyperthyroidism was induced by alternate day intraperitoneal injection of T_3 (3,3',5,triiodo-L-thyronine), 50 μg/100 g body weight as previously described (15). Untreated hypothyroid rats consumed chow–0.1% PTU for 21–28 days, while control euthyroid rats consumed unmodified rat chow. All groups were studied, as previously described (15), after a 16–18 h fast.

In vivo radiolabeling protocol

Animals were anesthetized with sodium pentobarbital and administered an intraportal vein bolus of 1 mCi L-[4,5^{3}H]leucine. After 15 min animals were exsanguinated and the liver was perfused in situ for 15 min with 100 ml ice-cold PBS–20 mM leucine containing freshly added PMSF (1 mM). In experiments where apoB biosynthesis alone was to be determined, liver samples were homogenized in PBS–1% Triton–2 mM leucine containing freshly added protease inhibitors at the indicated final concentrations: PMSF (1 mM), benzamidine (1 mM), leupeptin (100 μM), EDTA (5 mM), aprotinin (450 μM), pepstatin (2 μM), TLCK (25 μM). A 225,000 *g* supernatant was then prepared and stored at −80°C until used for immunoprecipitation.

Preparation of Golgi membrane fractions

After in vivo radiolabeling, livers from five to eight animals per group were pooled, minced, and homogenized on ice in five volumes 0.25 M sucrose–10 mM HEPES, pH 7.4, containing 1 mM PMSF, using a motor-driven Teflon Potter-Elvehjem apparatus. From this homogenate hepatic subcellular membrane fractions were prepared using modifications of the protocol of Ehrenreich et al. (16) as suggested by Howell and Palade (17). Briefly, the cellular homogenate was centrifuged at 10,000 *g*-av for 10 min, producing a pellet (P1) and supernatant (S1). S1 was reconstituted back to the original volume with 0.25 M sucrose–10 mM HEPES– 1 mM PMSF and centrifuged at 105,000 *g*-av for 90 min. The resultant supernatant (S2) was collected and stored at 80°C while the resultant microsomal pellet (P2) was resuspended in 0.25 M sucrose–10 mM HEPES–1 mM PMSF using a loose-fitting Teflon pestle. The P_2 suspension was adjusted to a sucrose concentration of 1.22 M using 2.0 M sucrose. Aliquots of 10 ml were loaded under a discontinuous gradient with 8.5-ml steps of 1.15 M, 0.86 M, and 0.25 M sucrose. This gradient was then centrifuged at 82,500 *g*-av for 180 min. Material accumulating at the 0.25 M/0.86 M interface, 0.86 M/1.15 M interface, 1.15 M/1.22 M interface, and the residual pellet were collected individually and are referred to as G_1, G_2, G_3, and G_4 fractions, respectively. The identity of these microsomal membrane fractions, at least in control animals, corresponds to Golgi vesicles (G_1), Golgi cisternae (G_2), and the remaining microsomal membrane fractions (G_3, G_4). All fractions were stored at −80°C until analysis. In some experiments, membranes were subjected to hypotonic lysis by incubation in 0.1 M Na_2CO_3 on ice, followed by neutralization and preparative ultracentrifugation to recover VLDL. Recovery of total protein in each fraction, in all the study groups (control, hypothyroid and hyperthyroid), was comparable (**Table 1**). Additionally, enrichment of G_1 and G_2 fractions for galactosyltransferase activity (18) was 17- to 70-fold over homogenate, with no

TABLE 1. Total protein recovery in subcellular fractions of rat liver

Fraction	Experimental Group		
	Control	Hypothyroid	Hyperthyroid
	mg	*mg*	*mg*
Homogenate	937.1 ± 129.5	1028.4 ± 247.3	1034.1 ± 100.1
S_1	553.9 ± 46.2	426.1 ± 112.8	497.0 ± 486.2
P_1	319.6 ± 46.1	324.3 ± 164.8	432.1 ± 89.2
S_2	241.8 ± 62.6	267.5 ± 83.2	295.8 ± 115.0
P_2	157.9 ± 57.3	117.9 ± 25.2	162.8 ± 20.8
G_1	5.6 ± 1.3	4.0 ± 0.7	4.8 ± 0.8
G_2	5.8 ± 1.3	5.0 ± 0.7	6.5 ± 0.5
G_3	28.9 ± 4.3	28.1 ± 5.3	29.8 ± 8.6
G_4	114.8 ± 5.8	92.4 ± 8.6	100.2 ± 7.2

Total protein mass (mg) was determined on sequential isolates from livers prepared from five to eight animals per group. The designations S_1, P_1 refer to the supernatant and pellet from the first 10,000 *g* centrifugation; S_2, P_2 refer to the supernatant and pellet resulting from recentrifugation (of S_1) at 105,000 *g*; G_1, G_2, G_3 refer to fractions isolated from the 0.25 M/0.86 M, 0.86 M/1.15 M, and 1.15 M/1.22 M sucrose interface, respectively, after discontinuous gradient ultracentrifugation (of P_2), while G_4 is the residual, final pellet (See Methods).

significant differences between control, hypothyroid, and hyperthyroid animals (data not shown). The G_1 fraction (which corresponds to that fraction designated GF_{1+2} by Ehrenreich et al. (16) and GF by Howell and Palade (17)) contained 13–35% of the total galactosyltransferase activity in the three groups, suggesting substantial enrichment of this fraction in Golgi vesicles.

Analysis of hepatic apoB protein

Immunoprecipitation of newly synthesized apoB was as previously described from samples made 1% with respect to Triton X-100 (19). Samples were subjected to exhaustive immunoprecipitation, as previously described (19), to insure complete recovery of immunoreactive apoB. The immune complexes were washed extensively and analyzed by denaturing SDS-PAGE on 4% acylamide disk gels which were sliced and assayed by liquid scintillation spectrometry (19). The migration of radiolabeled apoB-100 and apoB-48 was verified by reference to the mobility of these species in samples of coelectrophoresed rat serum VLDL.

The mass distribution of apoB variants was determined in aliquots of membrane fractions, nascent intracellular Golgi VLDL, and whole unfractionated serum as follows. Samples (0.5 –200 μg total protein or 0.5–1 μl serum) were prepared by incubation in 2% SDS–0.5% NP-40, on ice and without reduction or heating at any time. Samples were applied to a 5% acrylamide (20) slab gel and electrophoresed at 200 v for 30 min and 35 v for 16–20 h at 4°C. The samples were subsequently transferred to PVDF membranes (Millipore, Bedford, MA) in 25 mM Tris–192 mM glycine–10% (v/v) methanol at 100 v for 4–6 h at 4°C. The membranes were blocked by washing five times in PBS–0.3% Tween 20 at 37°C for 5 min each, and stained with india ink. Prior to immunostaining, the membranes were reblocked with Blotto buffer (5% nonfat dry milk–0.01% antifoam–0.5% Tween 20–0.2% sodium azide) at room temperature for 30 min and subsequently incubated with anti-rat apoB antiserum (1:1000–1:5000 dilution) in Blotto buffer for 2 h at room temperature. Blots were washed five times with TTBS (10 mM Tris, 0.15 M NaCl, 0.05% Tween 20, pH 7.5) for 5–10 min and incubated with ^{125}I-labeled protein A (ICN, 36 μCi/μg, final concentration 0.3 μCi/ml) for 30 min at room temperature. After five additional washes with TTBS, the blots were subjected to autoradiography and scanned by laser densitometry (LKB Ultroscan, Gaithersburg, MD).

Analysis of hepatic apoB messenger RNA

Hepatic RNA was extracted using 5 M guanidine isothiocyanate as described (21). Total apoB mRNA abundance was determined after dot-blot hybridization of aliquots of total RNA (15) using a 660 base pair cDNA fragment spanning nucleotides 6280–6940 of rat apoB cDNA. Hybridization and washing stringencies have been previously detailed (15). For analysis of the proportions of modified (B-STOP, UAA) to unmodified (B-GLN, CAA) apoB transcripts, total RNA was subjected to digestion with RNase-free DNase (RQ-1, Promega, WI) 1 U/μg RNA, followed by restriction digestion of any residual genomic DNA with Alu 1. The RNA was extracted with phenol–chloroform and precipitated with ethanol. Aliquots (1 μg) were reverse-transcribed using 200 U MMLV reverse transcriptase (BRL) in a buffer containing (final concentration) 50 mM KCl, 20 mM Tris, pH 8.4, 2.5 mM $MgCl_2$, 1 mg/ml acetylated bovine serum albumin, 100 pmol random hexamers, 10 mM dNTPs and 40 U RNA-sin (Promega). After first strand cDNA synthesis, a 274 base pair fragment was amplified by means of the polymerase chain reaction (PCR). Oligonucleotide primers were constructed to both coding (pcr 1) and noncoding (pcr 3) sequences flanking nucleotide 6666 of apoB cDNA: pcr 1: ATCTGACTGGGAGAGAC AAGTAG, 23-mer 5' at 6512; pcr 3: CACGGATATGA TACTGTTCGTCAAGC, 26-mer 5' at 6786. PCR was conducted as previously described using 1 μM concentration of each primer and 2.5 uTaq polymerase (Perkin-Elmer-Cetus, Norwalk, CT) (6) with the following modifications: final concentrations of 20 mM Tris, 1.7 mM $MgCl_2$ and 1 mg/ml acetylated bovine serum albumin, the latter replacing gelatin (6). Denaturation was conducted at 94°C for 30 sec, annealing at 55°C for 1 min, and extension at 72°C for 90 sec, a total of 25 cycles with a final 10-min extension at 72°C. PCR products were analyzed by 3 GTG-1% Seakem agarose electrophoresis to confirm the size of the amplified product

and dilutions were subsequently made for direct application to nitrocellulose membranes and differential hybridization with oligonucleotides BGLN TACTGATCAAATTG* TATCA, 19 mer 5' end at 6679 and B STOP TACTGAT CAAATTA*TATCA 19-mer 5', and at 6679 as previously detailed (6). Washes were carried out using 3 M tetramethylammonium chloride–50 mM Tris-HCl, pH 8.0,–2 mM EDTA–0.01% SDS at 46°C and 48°C (6).

Miscellaneous assays

Total protein was determined as previously described (22); protein mass in nascent Golgi VLDL was determined using colloidal gold (23). Golgi VLDL were visualized by negative stain electron microscopy after staining with 2% phosphotungstic acid, pH 7.2. Sizing of particles was undertaken using a Nikon Shadowgraph (Model 6C) equipped with a digital readout. Immunological detection of LDL-receptor protein in membrane fractions of rat livers (10,000–105,000 *g*) was undertaken using nonreducing sample preparation conditions (detailed above) with a 7.5% acrylamide separating/3% acrylamide stacking gel. Antiserum to rat LDL-receptor protein was used at a 1:1000 dilution and was generously provided by A. D. Cooper, Palo Alto Medical Foundation, Palo Alto, CA. Statistical comparisons were made using independent *t*-tests and used both pooled and separated variance analysis where appropriate. Data, unless otherwise stated, are expressed as mean ± SD.

RESULTS

Distribution of newly synthesized apoB-100 and B-48 among subcellular membrane fractions

Studies in control and hypothyroid animals. Analysis of the distribution of newly synthesized apoB species among microsomal membrane subfractions from discontinuous sucrose gradients in both control and hypothyroid animals revealed a predominance of apoB-100 (**Fig. 1**). Specifically, membranes isolated at the 0.25 M/0.86 M sucrose interface (G_1) were found to contain 93–95% total newly synthesized apoB as apoB-100, while membranes isolated at the 0.86 M/1.15 M sucrose interface (G_2) were found to contain 87 ± 7% apoB-100 in hypothyroid animals and exclusively apoB-100 in all control animals (Fig. 1). ApoB-100 represented 33–45% of total newly synthesized apoB in the remaining microsomal membrane fractions (G_3, G_4) from both groups.

Studies in hyperthyroid animals. Our earlier observations (15), confirmed in the present study group, demonstrated that radiolabeled liver homogenate samples from hyperthyroid animals, prepared by Polytron disruption in Triton-containing buffers (with freshly added protease inhibitors), contained no detectable apoB-100 immunoreactive product (<0.03% total protein synthesis, data not shown). The present studies provide more critical resolution of these findings by demonstrating that while apoB-48 represented the predominant newly synthesized apoB species among microsomal membrane subfractions from hyperthyroid animals, newly synthesized apoB-100 was readily detectable, representing 46 ± 10% of total newly synthesized apoB in the G_1 fraction, and 24 ± 11% in the G_2 fraction (Fig. 1).

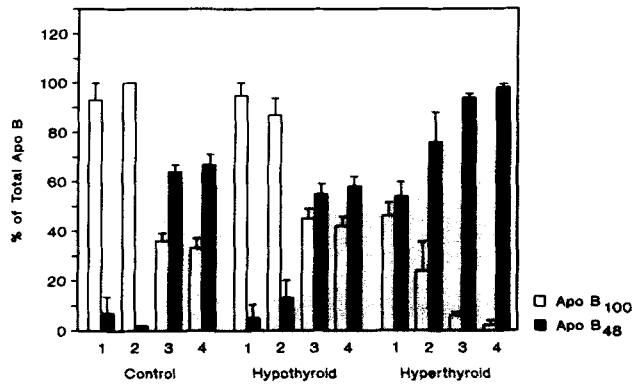

Fig. 1. ApoB synthesis in subcellular membrane fractions of rat liver. Animals were subjected to hormonal manipulations as detailed in Methods. In vivo radiolabeling was undertaken by intraportal vein administration of 1 mCi L-[4,5-^{3}H]leucine for a 15-min pulse after which livers were perfused in situ for an additional 15 min with PBS–20 mM leucine. Livers were removed, homogenized in 0.25 M sucrose–10 mM HEPES, and subjected to sequential centrifugation at 10,000 *g* and 105,000 *g* followed by separation of the 105,000 *g* pellet through a discontinuous sucrose gradient (Methods). Fractions collected at the respective interfaces (G_1, G_2, G_3) were removed by aspiration and the residual pellet (G_4) was collected and stored at −80°C until analysis. All fractions were made 1% with respect to final Triton X-100 concentration and newly synthesized apoB species were recovered by quantitative immunoprecipitation. ApoB-100 and apoB-48 were resolved on denaturing 4% SDS-PAGE and quantitated by gel slicing and liquid scintillation spectrometry. The data for apoB-100 (□) and apoB-48 (■) are expressed as a percent of total immunoreactive apoB species, with standard error. The experiments reported are from four to six immunoprecipitations each from four animals per group.

It bears emphasis that, in the current study group, similar yields were obtained of total homogenate protein (Table 1) and at similar specific activity (TCA precipitable counts per μg) to our previously published values (control 179 ± 39 cpm/μg, hyperthyroid 110 ± 19 cpm/μg compared 169 ± 61 and 122 ± 42 cpm/μg for control and hyperthyroid animals previously characterized by our laboratory (15)). Additionally, hepatic apoB-100 synthesis rates, determined by immunoprecipitation of homogenate fractions from hyperthyroid animals, prepared by Teflon-glass homogenization in 0.25 M sucrose, were substantially reduced by comparison with both control and hypothyroid animals (0.05 ± 0.06 vs control 0.29 ± 0.14 and hypothyroid 0.30 ± 0.19% total protein, n = 4 per group, $P<0.01$). ApoB-48 synthesis rates were indistinguishable in hypothyroid and hyperthyroid animals (0.40 ± 0.15 and 0.42 ± 0.10% total protein respectively, n = 4, $P>0.05$), findings analogous to previous data

TABLE 2. Relative specific activity and distribution of newly synthesized apo B species among microsomal membrane subfractions

	Experimental Group					
	Control		Hypothyroid		Hyperthyroid	
Fraction	B-100	B-48	B-100	B-48	B-100	B-48
G_1	2250 ± 700 (6.7 ± 1.6)	1800 ± 310 (0.3 ± 0.5)	830 ± 100 (5.4 ± 1.6)	180 ± 320 (0.9 ± 1.5)	810 ± 260 (53.7 ± 11.9)	1160 ± 510 (2.6 ± 0.8)
G_2	780 ± 380 (2.4 ± 0.4)	N.D. (0)	530 ± 50 (4.3 ± 0.5)	80 ± 80 (0.6 ± 0.7)	60 ± 60 (5.3 ± 4.7)	470 ± 310 (1.5 ± 0.9)
G_3	990 ± 240 (17.4 ± 3.5)	1690 ± 290 (15.9 ± 1.3)	540 ± 320 (22.6 ± 9.8)	620 ± 250 (21.8 ± 9.1)	90 ± 30 (40.8 ± 8.3)	1370 ± 470 (20.2 ± 3.8)
G_4	1160 ± 460 (73.8 ± 5.0)	2250 ± 200 (83.8 ± 1.0)	440 ± 90 (67.6 ± 9.1)	630 ± 190 (75.3 ± 10.4)	N.D. (0)	1440 ± 330 (75.6 ± 2.5)

Livers from control, hypothyroid, and T_3 hyperthyroid animals were pulse labeled, in vivo, as described above (Methods). Livers were subjected to sequential isolation of intracellular membrane fractions by discontinuous sucrose gradient centrifugation of the 105,000 *g* membrane pellet (Methods). ApoB-100 and B-48 specific activity was determined by quantitative immunoprecipitation followed by SDS-PAGE to resolve each isomorph. The data are expressed as cpm immunoprecipitable apoB normalized to membrane protein content (cpm/mg). Each value represents the mean ± SD from four to six immunoprecipitations on samples from four animals per group. Values in parentheses refer to the percent distribution of newly synthesized apoB between the respective microsomal membrane subfractions; ND, no immunoprecipitable apoB counts detected.

(15). Furthermore, analysis of hepatic RNA from the current study group showed T_3-dependent modulation of apoB mRNA editing indistinguishable from our earlier report (6), with control and hypothyroid animals demonstrating a range of 45–84% unmodified apoB (B-GLN) and a mean of 50–61% B-GLN while hyperthyroid animals were found to have only 6 ± 1% B-GLN. Taken together, the data suggest that hyperthyroid rat liver continues to synthesize apoB-100, albeit at a reduced rate, and that this apoB variant is relatively abundant (as demonstrated below) in a discrete membrane fraction (G_1), following tissue homogenization and subcellular fractionation in detergent-free buffers.

Specific activity and experimental recovery of newly synthesized apoB-100 and B-48

As demonstrated in **Table 2**, apoB-100 specific activity was maximal in the G_1 fraction from all groups examined, a trend most clearly evident in hyperthyroid animals. Furthermore, the distribution of newly synthesized apoB-100 among the microsomal membrane subfractions (Table 2) revealed that the G_1 fraction accounted for 40–62% of the total (microsomal) apoB-100 counts in hyperthyroid animals, while in control and hypothyroid animals, apoB-100 counts in the G_1 fraction accounted for only 4–8% of the total. In these latter two groups, 57–79% of newly synthe-

TABLE 3. Recovery of newly synthesized apo B in subcellular fractions of rat liver

	Experimental Group					
	Control		Hypothyroid		Hyperthyroid	
Fraction	B-100	B-48	B-100	B-48	B-100	B-48
Homogenate	1.0	1.0	1.0	1.0	1.0	1.0
$S_1 + P_1$	0.89 ± 0.25	0.72 ± 0.36	1.29 ± 0.35	0.60 ± 0.21	0.69 ± 0.24	0.99 ± 0.15
S_1	1.0	1.0	1.0	1.0	1.0	1.0
$(S_1 + P_2)$	0.68 ± 0.02	0.71 ± 0.02	0.97 ± 0.44	0.79 ± 0.31	1.24 ± 0.49	1.17 ± 0.19
P_2	1.0	1.0	1.0	1.0	1.0	1.0
$(G_1 + G_2 + G_3 + G_4)$	1.07 ± 0.24	0.99 ± 0.26	0.79 ± 0.21	0.91 ± 0.26	0.20 ± 0.06[a]	0.67 ± 0.10

Livers from control, hypothyroid, and T_3-treated hyperthyroid animals were pulse-labeled in vivo as described in Methods. Livers were subjected to sequential isolation of intracellular fractions (S_1, P_1; S_2, P_2; G_1, G_2, G_3, G_4) as described (Methods) and radiolabel incorporation into newly synthesized apoB-100 and apoB-48 was determined following quantitative immunoprecipitation and analytical SDS-PAGE. Gels were sliced and radioactivity was determined on individual slices by scintillation counting. Migration of apoB-100 and apoB-48 was determined by reference to coelectrophoresed rat serum VLDL. The abbreviations used (S_1, P_1, etc.) are defined in detail above (Methods). The data are expressed as a fractional recovery for each of the three sequential centrifugation steps. Each value represents the mean ± SD of four to six immunoprecipitations on samples from four animals per group.

[a]Recovery of apoB-100 is significantly lower than from control or hypothyroid animals, $P < 0.001$. There were no other significant differences in apoB recovery.

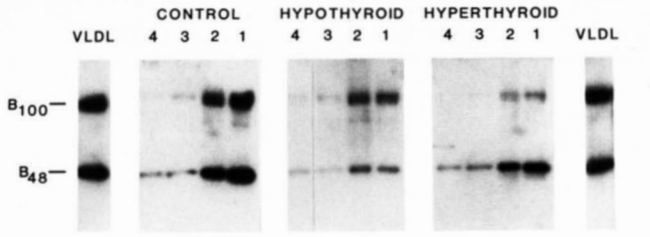

Fig. 2. ApoB mass distribution in subcellular membrane fractions of rat liver. Rat liver membrane fractions were prepared as detailed in Methods and the legend to Fig. 1, after discontinuous sucrose gradient centrifugation. Fifty μg total protein from each fraction was suspended in 2% SDS–0.5% NP-40 without reduction, prior to loading onto a 5% acrylamide slab gel (Methods). Samples were electrophoresed for approximately 800 volt-hours, transferred to a PVDF membrane, and immunostained with anti-rat apoB and ^{125}I-labeled protein A. Rat serum VLDL was coelectrophoresed as a marker of apoB-100 and B-48 migration. This is a representative example from four replicate experiments.

sized apoB-100 was present in the residual pellet (G_4). By contrast, the G_4 fraction from hyperthyroid animals was repeatedly extracted without releasing detectable apoB-100 immunoreactive material (Table 2). Additionally, no lower molecular weight (apoB) fragments were detectable (data not shown). The distribution of newly synthesized apoB-48 revealed that less than 4% was found in G_1 fractions with the majority (63–84%) recovered in the G_4 fractions.

The overall experimental recovery of newly synthesized apoB species is illustrated in **Table 3**. Recovery of newly synthesized apoB-100 and B-48 was comparable in control and hypothyroid animals. By contrast, recovery of newly

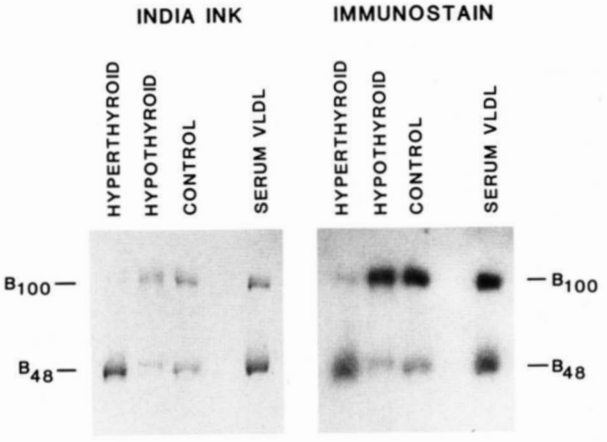

Fig. 3. ApoB mass distribution in intracellular nascent VLDL from subcellular membrane fractions of rat liver. Subcellular membrane fractions were prepared from five to eight rat livers as outlined in the legend to Fig. 1 and Methods, after discontinuous sucrose gradient centrifugation. Five hundred ng total protein from G_1 fractions (isolated at the 0.25 M/0.86 M sucrose interface) was suspended in 2% SDS- 0.5% NP-40 without reduction, prior to loading onto a 5% acrylamide slab gel (Methods). Samples were electrophoresed for approximately 800 volt-hours, transferred to a PVDF membrane, and stained sequentially with India ink and anti-rat apoB antiserum followed by ^{125}I-labeled protein A (Methods). Rat serum VLDL was coelectrophoresed as a marker of apoB-100 and B-48 migration.

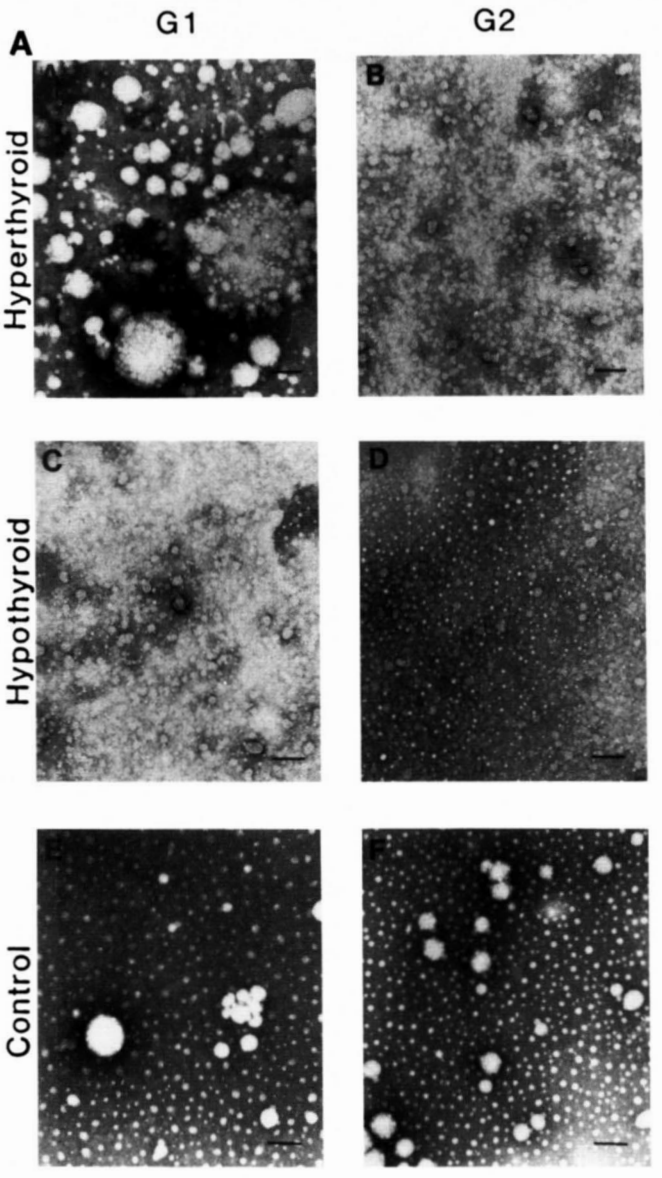

synthesized apoB-100 in hyperthyroid animals was consistently reduced (20 ± 6%) following resuspension of the microsomal pellet and discontinuous sucrose gradient fractionation (Table 3). This apparently selective loss of newly synthesized apoB-100 and the underlying mechanism(s) responsible will require further study.

Mass distribution of apoB-100 and B-48 among subcellular membrane fractions

Aliquots of membrane fractions were analyzed by 5% SDS-PAGE followed by Western blotting and the results of a representative immunoblot experiments are presented in **Fig. 2**. Control animals demonstrated that 44–47% of the apoB mass in fractions G_1 and G_2 was apoB-100 while these same fractions from hypothyroid animals demonstrated 57–71% apoB-100. The correspond-

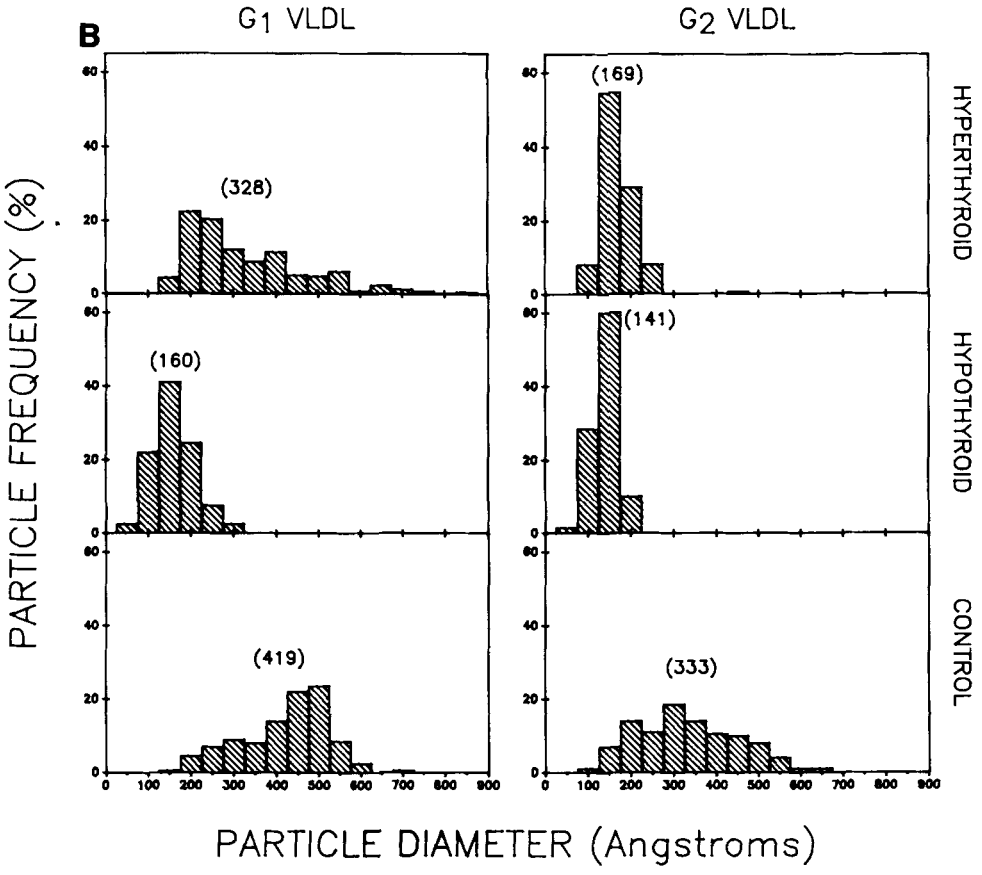

Fig. 4. A: Nascent intracellular VLDL. Subcellular membrane fractions, prepared from control (euthyroid), hypothyroid, and hyperthyroid animals as detailed in Methods, were subjected to hypotonic, sodium carbonate lysis. VLDL were isolated by ultracentrifugation at $d < 1.006$ g/ml and visualized by negative staining after incubation with 2% phosphotungstic acid, pH 7.2. Nascent VLDL from hyperthyroid animals are displayed in panels A (G_1) and B (G_2), from hypothyroid animals in panels C (G_1) and D (G_2), and from control animals in panels E (G_1) and F (G_2). The magnification is × 34,000 and the bar represents 1,000 Å. B: Histogram of nascent intracellular VLDL. Two hundred or 300 particles from each group were sized and the distribution of each VLDL preparation is displayed. The mean diameter for the group is shown in parentheses above the frequency bars. G_1 and G_2 refer to membrane fractions isolated at the 0.25 M/0.86 M interface and 0.86 M/1.15 M sucrose interface, respectively (Methods).

ing G_1 and G_2 fractions from hyperthyroid animals contained 75–90% of apoB mass as apoB-48 (Fig. 2). Thus, in all groups, steady-state mass distribution of apoB variants differs from the ratio of newly synthesized apoB peptides, suggesting that the intracellular metabolism (possibly including compartmentation and degradation) of each apoB species is independently regulated and appears to be influenced by changes in thyroid hormone status.

Nascent intracellular VLDL: apoB distribution and particle morphology

A further group of experiments was undertaken to examine whether alterations in hepatic apoB gene expression and intracellular distribution of apoB species are associated with changes in the relative apoB composition and morphology of nascent VLDL. ApoB mass distribution in nascent VLDL from G_1 fractions is illustrated in **Fig. 3**. The results suggest that apoB-100 in nascent VLDL from control and hypothyroid livers accounts for 70–78% total apoB species. These data for apoB mass distribution in control and hypothyroid nascent VLDL are thus qualitatively similar to the biosynthetic data presented above (Fig. 1) By contrast, apoB composition in nascent VLDL from hyperthyroid livers was approximately 78% apoB-48, as compared to 54% apoB-48, as determined by biosynthetic analysis (see Fig. 1). These data imply that apoB-48 is preferentially incorporated into nascent VLDL in hyperthyroid rat liver despite the presence of (small amounts) of apoB-100, as evidenced by

the biosynthetic data. Direct visualization of nascent VLDL (**Fig. 4**) from the respective groups shows a heterodisperse morphology and similar size range between VLDL isolated from G_1 membranes of hyperthyroid and control animals (Fig. 4A, 4B). VLDL from the G_1 fraction of hypothyroid animals, by contrast, were smaller (mean 160 Å vs 328 Å in hyperthyroid and 419 Å in control) and monodisperse (Fig. 4B). Particles isolated from G_2 membranes of hypothyroid and hyperthyroid animals were of similar size distribution and were both smaller and relatively monodisperse in comparison to G_2 VLDL isolated from control animals. No VLDL particles were recovered from G_3 and G_4 fractions following sodium carbonate extraction (data not shown).

Previous studies demonstrated a reduction in serum apoB-100 levels in T_3-treated animals which likely reflects the reduction in apoB-100 synthesis but additionally, may reflect alterations in apoB catabolism, as previously suggested (24). Evidence for this is suggested in **Fig. 5** which shows that liver membranes from hyperthyroid animals demonstrated an increase in immunodetectable LDL-receptor protein. Specifically, there was a threefold increase in the 130 kDa form, which was the predominant immunoreactive species identified in all groups. Additionally, however, a form of 190 kDa was readily detectable in membranes from hyperthyroid animals and appeared approximately tenfold more abundant than in membranes from hypothyroid animals (Fig. 5). The cumulative evidence thus provides direct support for both decreased production of apoB-100 and augmented apoB-100 clearance as a result of T_3 administration.

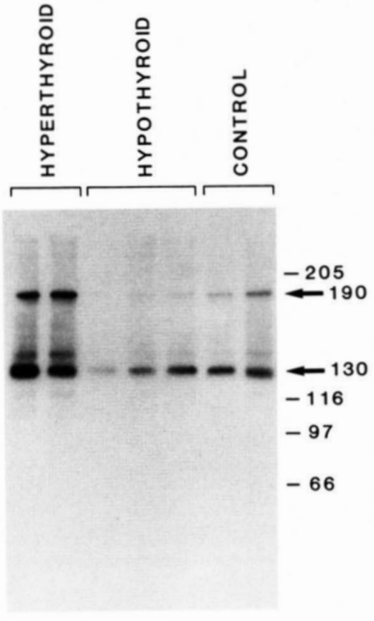

Fig. 5. Anti-LDL-receptor immunostaining of rat liver membrane fractions: effects of thyroid hormone modulation. Fifty μg total protein from the 10,000–105,000 *g* liver membrane fraction was suspended in 2% SDS–0.5% NP-40 and electrophoresed on a 7.5% acrylamide slab gel (Methods). After transfer to a PVDF membrane, the blot was immunostained with polyclonal anti-rat LDL receptor antibody and ^{125}I-labeled protein A (Methods). Coelectrophoresed high molecular weight markers were visualized by India ink staining, and are shown on the right. The calculated molecular weights of the two major immunoreactive bands (heavy arrows) correspond to 190 and 130 kDa.

DISCUSSION

The major conclusions of this work are that T_3-dependent modulation of hepatic apoB-100 mRNA editing is associated with alterations in the biosynthesis and distribution of apoB-100 and apoB-48 among microsomal membrane subfractions and in nascent Golgi VLDL. Several aspects of these conclusions merit further review.

The results of the biosynthetic labeling experiments in control animals confirm previous studies examining the temporal relationship of apoB-100 and apoB-48 biosynthesis in Golgi membrane fractions (10). Specifically, the current demonstration of a predominance of newly synthesized apoB-100 in G_1 membrane fractions with the inverse situation (i.e., apoB-48 predominance) in the G_3 and G_4 fractions in control and hypothyroid animals, is consistent with the suggestion (12, 13) that the movement of these two variants from their site of synthesis into membrane domains (which may be involved in VLDL assembly) is independently regulated. Evidence for this is provided by the results of the biosynthetic labeling study which contrast with the results obtained by Western blot analysis of these same membrane fractions. Specifically, in G_1 and G_2 membrane fractions from control animals, apoB-100 represented virtually 100% of newly synthesized apoB species but only 44–47% of apoB mass. Similarly, the G_1 and G_2 membrane fractions from hyperthyroid animals were relatively enriched in apoB-48 mass (75–90% total apoB as determined by Western blotting) as compared to the results of the biosynthetic study (54–75% total apoB). These observations are consistent with the temporal delay in appearance of newly synthesized apoB-48 in Golgi membranes previously described after in vivo pulse-radiolabeling (10). Specifically, these studies demonstrated maximal labeling of newly synthesized apoB-100 15 min after isotope administration (identical to the current radiolabeling protocol) while apoB-48 achieved maximal labeling after 30 min (10). An alternative, but less likely, explanation for the divergence between biosynthetic and mass ratios of apoB-100 and B-48 is that the G_1 and G_2 membrane fractions may be enriched in apoB-48 by virtue of contamination with endocytic components such as multivesicular bodies (MVBs) containing predominantly apoB-48 (25). While not specifically addressed in the present studies, other workers using similar separation techniques to those used here

have raised this possibility and concluded experimentally that such contamination was likely to be insignificant (10, 26). Specifically, these workers found that less than 1% of the injected ^{125}I-labeled VLDL or ^{125}I-labeled LDL was recovered in Golgi membrane fractions (10, 26). Furthermore, the original description of MVB contamination of Golgi membrane fractions demonstrated that only 1.6% of the injected ^{125}I-labeled LDL recovered in homogenate fractions could be found in Golgi membranes compared to 12.1% for the MVB fraction (Table 2 of reference 25). The demonstration of increased immunodetectable LDL-receptor protein in liver membrane fractions from hyperthyroid animals (Fig. 5) does, however, raise the question of whether alterations in lipoprotein catabolism could contribute to the changes in intracellular apoB distribution. This same polyclonal antibody identified several reactive species on Western blots of sucrose gradient-isolated membrane fractions from both control and hyperthyroid animals, including a principal species of 130 kDa which appeared of similar intensity in membranes isolated from control and hyperthyroid groups (Davidson, N. O., unpublished results). These observations are consistent with the recent demonstration of several lipoprotein-binding species in rat liver Golgi membrane fractions, although in this latter report the abundance of this 130 kDa species was increased several-fold after ethinylestradiol treatment (26, 27). Inasmuch as this estrogen-inducible LDL receptor may contribute to the catabolic clearance of chylomicron and VLDL remnants (27), it remains possible that contamination of the G_1 and G_2 membranes with endosomes containing this receptor-ligand complex could result in apparent enrichment of apoB-48 protein. However, in the present context, this issue is currently unresolved.

The results of the present study demonstrate evidence for active apoB-100 biosynthesis in hyperthyroid rat liver. Specifically, apoB-100 synthesis was reduced, although detectable, in homogenate samples prepared by glass-Teflon mechanical homogenization in 0.25 M sucrose. However, apoB-100 synthesis was undetectable in either homogenate samples or 225,000 *g* supernatant fractions prepared from hyperthyroid livers using Polytron disruption in Triton X-100 containing buffers. These observations raise the possibility that homogenization conditions and the presence of detergents may somehow influence the stability or immunoreactivity of nascent apoB-100 in hyperthyroid liver. In support of this general possibility is the observation that the recovery of newly synthesized apoB-100 was dramatically reduced (20%) in hyperthyroid liver samples after resuspension of the 105,000 *g* pellet and discontinuous sucrose gradient centrifugation (Table 3). This apparently selective loss of nascent apoB-100 in hyperthyroid rat liver membrane fractions is compatible with the recent proposal that discrete intracellular sites of apoB degradation exist and may play a role in regulating VLDL assembly (12, 13). The biochemical nature and location of such a process, however, remain to be determined. Continued biosynthesis of apoB-100 in hyperthyroid rat liver is internally consistent with the results of the apoB-100 mRNA editing analysis, undertaken using hepatic RNA from these same animals. The data indicate that 6 ± 1% of the PCR products contain the unmodified (B-GLN, CAA) apoB cDNA, a value identical to that previously reported (6). In light of the detection of newly synthesized apoB-100 in hyperthyroid rat liver samples prepared by homogenization in 0.25 M sucrose, the question must be readdressed as to whether active biosynthesis of apoB-100 can be demonstrated in adult mammalian enterocytes, where apoB-100 mRNA editing occurs to a similar extent as reported above. Our own (19) and other data (28) have demonstrated that radiolabeled intestinal homogenates from the adult rat, prepared by either Polytron disruption in Triton X-100-containing buffers or nitrogen cavitation, contain no immunoreactive newly synthesized apoB-100. However, the possibility exists that the (presumably small) amounts of apoB-100 synthesized may be rapidly degraded in the presence of detergents and this issue is currently under investigation.

The morphology and size distribution of the nascent VLDL isolated from the G_1 and G_2 membrane fractions of control animals are similar to those reported by Dolphin (29) and Dolphin and Forsyth (30). The relative protein distribution of apoB species as determined by Western blotting revealed a predominance of apoB-100 in both control and hypothyroid animals, consistent with previous reports of the apoB-100/B-48 ratio in liver perfusate VLDL from fasted animals (9). Nascent VLDL isolated from the G_1 membrane fractions of hyperthyroid animals demonstrated a clear predominance of apoB-48, a finding which, taken together with the apparently normalized morphology and size distribution (compared to untreated, hypothyroid animals), suggests that VLDL assembly and secretion may proceed in the relative absence of apoB-100. Although this remains to be shown directly in hyperthyroid animals, the available evidence suggests that hepatic VLDL in the rat are assembled with a single apoB peptide and that the majority of VLDL particles from control animals contain apoB-48 as the sole apoB species (31). Since we have previously demonstrated that hepatic triglyceride synthesis and secretion are normalized following T_3 administration to hypothyroid rats (15), we speculate that apoB-48 alone contains sufficient conformational competence to direct effective assembly of hepatic VLDL.

Dr. Davidson was supported by NIH grant HL-38180, an American Heart Association Grant-in-Aid (88-1015), and a Research Career Development Award K04 HL02166. R. Carlos was supported in part by a Summer Student Research Fellowship Award from the American Gastroenterological Association. H. Sherman received a predoctoral training grant from

NIH (HD-07009). Dr. Hay was supported by grants from NHLBI (SCOR-Atherosclerosis 15062), the American Heart Association (85-805), and the Louis Block Fund. The authors acknowledge the assistance of Mrs. P. Cantwell in preparation of this manuscript and the helpful comments of Dr. B. Teng. In addition, the authors acknowledge the generous assistance of Dr. Robert Josephs in preparation of the electron micrographs and Dr. Allen Cooper for providing anti-LDL receptor antiserum.

Manuscript received 29 September 1989, in revised form 5 December 1990, and in re-revised form 27 December 1989.

REFERENCES

1. Li, W-H., M. Tanimura, C-C. Luo, S. Datta, and L. Chan. 1988. The apolipoprotein multigene family: biosynthesis, structure, structure-function relationships, and evolution. *J. Lipid Res.* **29:** 245-271.
2. Powell, L. M., S. C. Wallis, R. J. Pease, Y. H. Edwards, T. J. Knott, and J. Scott. 1987. A novel form of tissue-specific RNA processing produces apolipoprotein B-48 in intestine. *Cell.* **50:** 831-840.
3. Chen S-H., G. Habib, C-Y. Yang, Z-W. Gu, B. R. Lee, S-A. Weng, S. R. Silberman, S-J. Cai, J. P. Deslypere, M. Rossenue, A. M. Gotto, Jr., W-H. Li, and L. Chan. 1987. Apolipoprotein B-48 is the product of a messenger RNA with an organ-specific in-frame stop codon. *Science.* **238:** 363-366.
4. Bell-Quint, J., T. Forte, and P. Graham. 1981. Synthesis of two forms of apolipoprotein B by cultured hepatocytes. *Biochem. Biophys. Res. Commun.* **99:** 700-706.
5. Elovson, J., Y. O. Huang, N. Baker, and R. Kannan. 1981. Apolipoprotein B is structurally and metabolically heterogeneous in the rat. *Proc. Natl. Acad. Sci. USA.* **78:** 157-161.
6. Davidson, N. O., L. M. Powell, S. C. Wallis, and J. Scott. 1988. Thyroid hormone modulates the introduction of a stop codon in rat liver apolipoprotein B messenger RNA. *J. Biol. Chem.* **263:** 13482-13485.
7. Tennyson, G. E., C. A. Sabatos, K. Higuchi, N. Meglin, and H. B. Brewer, Jr. 1989. Expression of apolipoprotein B mRNAs encoding higher- and lower-molecular weight isoproteins in rat liver and intestine RNA editing. *Proc. Natl. Acad. Sci. USA.* **86:** 500-504.
8. Sparks, J. D., C. E. Sparks, M. Bolognino, A. M. Roncone, T. K. Jackson, and J. M. Amatruda. 1988. Effects of nonketotic streptozotocin diabetes on apolipoprotein B synthesis and secretion by primary cultures of rat hepatocytes. *J. Clin. Invest.* **82:** 37-43.
9. Windmueller, H. G., and A. E. Spaeth. 1985. Regulated biosynthesis and divergent metabolism of three forms of hepatic apolipoprotein B in the rat. *J. Lipid Res.* **26:** 70-81.
10. Swift, L. L., R. J. Padley, and G. S. Getz. 1987. Differential labeling of rat hepatic Golgi and serum very low density lipoprotein apoprotein B variants. *J. Lipid Res.* **28:** 207-215.
11. Reuben, M. A., K. L. Svenson, M. H. Doolittle, D. F. Johnson, A. J. Lusis, and J. Elovson. 1988. Biosynthetic relationships between the three rat apolipoprotein B peptides. *J. Lipid Res.* **29:** 1337-1347.
12. Borchardt, R. A., and R. A. Davis. 1987. Intrahepatic assembly of very low density lipoprotein. *J. Biol. Chem.* **262:** 16394-16402.
13. Davis, R. A., A. B. Prewett, D. C. F. Chan, J. J. Thompson, R. A. Borchardt, and W. R. Gallaher. 1989. Intrahepatic assembly of very low density lipoproteins: immunologic characterization of apolipoprotein B in lipoproteins and hepatic membrane fractions and its intracellular distribution. *J. Lipid Res.* **30:** 1185-1196.
14. Boström, K., J. Borén, M. Wettesten, A. Sjöberg, G. Bondjers, O. Wiklund, P. Carlsson, and S-O. Olofsson. 1988. Studies on the assembly of apoB-100-containing lipoproteins in HepG2 cells. *J. Biol. Chem.* **263:** 4434-4442.
15. Davidson, N. O., R. C. Carlos, M. J. Drewek, and T. G. Parmer. 1988. Apolipoprotein gene expression in the rat is regulated in a tissue-specific manner by thyroid hormone. *J. Lipid Res.* **29:** 1511-1522.
16. Ehrenreich, J. H., J. J. Bergeron, P. Siekevita, and G. E. Palade. 1973. Golgi fractions prepared from rat liver homogenates. I. Isolation procedure and morphological characterization. *J. Cell Biol.* **59:** 45-72.
17. Howell, K. E., and G. Palade. 1982. Hepatic Golgi fractions resolved into membrane and content subfractions. *J. Cell. Biol.* **92:** 822-832.
18. Hay, R., R. Fleming, W. O'Connell, J. Kirschner, and W. Oppliger. 1988. Apolipoproteins of the orotic acid fatty liver: implications for the biogenesis of plasma lipoproteins. *J. Lipid Res.* **29:** 981-995.
19. Davidson, N. O., M. E. Kollmer, and R. M. Glickman. 1986. Apolipoprotein B synthesis in rat small intestine: regulation by dietary triglyceride and biliary lipid. *J. Lipid Res.* **27:** 30-39.
20. Laemmli, U. K. 1970. Cleavage of structural proteins during the assembly of the head of bacteriophage T4. *Nature.* **227:** 680-685.
21. Han, J. H., C. Stratowa, and W. J. Rutter. 1987. Isolation of full-length putative rat lysophospholipase cDNA using improved methods for mRNA isolation and cDNA cloning. *Biochemistry.* **26:** 1617-1625.
22. Lowry, O. H., N. J. Rosebrough, A. L. Farr, and R. J. Randall. 1951. Protein measurement with the Folin phenol reagent. *J. Biol. Chem.* **193:** 265-275.
23. Stoscheck, C. M. 1987. Protein assay sensitive at nanogram levels. *Anal. Biochem.* **160:** 301-305.
24. Scarabottolo, L., E. Trezzi, P. Roma, and A. L. Catapano. 1986. Experimental hypothyroidism modulates the expression of the low density lipoprotein receptor by the liver. *Atherosclerosis.* **59:** 329-333.
25. Hornick, C. A., R. L. Hamilton, E. Spaziani, G. H. Enders, and R. J. Havel. 1985. Isolation and characterization of multivesicular bodies from rat hepatocytes: an organelle distinct from secretory vesicles of the Golgi apparatus. *J. Cell. Biol.* **100:** 1558-1569.
26. Harrison, J. C., L. S. Swift, and V. S. LeQuire. 1988. Identification of lipoprotein-binding proteins in rat liver Golgi apparatus membranes. *J. Lipid Res.* **29:** 1439-1449.
27. Cooper, A. D., R. Nutik, and J. Chen. 1987. Characterization of the estrogen-induced lipoprotein receptor of rat liver. *J. Lipid Res.* **28:** 59-68.
28. Magun, A. M., B. Mish, and R. M. Glickman. 1988. Intracelluar apoA-I and apoB distribution in rat intestine is altered by lipid feeding. *J. Lipid Res.* **29:** 1107-1116.
29. Dolphin, P. J. 1981. Serum and hepatic nascent lipoproteins in normal and hypercholesterolemic rats. *J. Lipid Res.* **22:** 971-989.
30. Dolphin, P. J., and S. J. Forsyth. 1983. Nascent hepatic lipoproteins in hypothyroid rats. *J. Lipid Res.* **24:** 541-551.
31. Elovson, J., J. E. Chatterton, G. T. Bell, V. N. Schumaker, M. A. Reuben, D. L. Puppione, J. R. Reeve, Jr., and N. L. Young. 1988. Plasma very low density lipoproteins contain a single molecule of apolipoprotein B. *J. Lipid Res.* **29:** 1461-1473.